Functional reorganization of brain networks across the human menstrual cycle

Laura Pritschet[1*], Tyler Santander[1*], Evan Layher[1], Caitlin M. Taylor[1], Shuying Yu[1], Michael B. Miller[1,2,3], Scott T. Grafton[1,2], & Emily G. Jacobs[1,2,3]

[1]Department of Psychological & Brain Sciences, University of California, Santa Barbara, USA
[2]Neuroscience Research Institute, University of California, Santa Barbara, USA
[3] Institute for Collaborative Biotechnologies, University of California, Santa Barbara, USA
[*]Authors contributed equally to this work.

Correspondence:
Emily G. Jacobs
Department of Psychological & Brain Sciences
University of California, Santa Barbara
Santa Barbara, CA 93106
emily.jacobs@psych.ucsb.edu

Key Words: sex hormones, estrogen, progesterone, menstrual cycle, fMRI, functional connectivity, brain networks, resting state

Abstract

Densely sampling the individual connectome could transform our understanding of the functional organization of the human brain. The brain is an endocrine organ, sensitive to cyclic changes in hormone production. However, the influence of sex hormones on the brain's intrinsic network architecture is largely unknown. Here, we examine the extent to which endogenous fluctuations in sex hormones alter functional brain networks at rest in a woman over 30 consecutive days. Time-synchronous analyses illustrate estrogen and progesterone's widespread influence on cortical dynamics throughout the cycle. Time-lagged analyses examined the temporal flow of these relationships and reveal estrogen's ability to drive connectivity across major functional networks, including the Default Mode and Dorsal Attention Networks, whose hubs are densely populated with estrogen receptors. These results reveal the rhythmic nature of brain network reorganization across the human menstrual cycle. Considering the hormonal milieu is critical for fully understanding the intrinsic dynamics of the human brain.

Introduction

The brain is an endocrine organ whose day-to-day function is intimately tied to the action of neuromodulatory hormones[1–4]. Yet, the study of brain-hormone interactions in human neuroscience has often been woefully myopic in scope: the classical approach of interrogating the brain involves collecting data at a single time point from multiple subjects and averaging across individuals to provide evidence for a hormone-brain-behavior relationship. This cross-sectional approach obscures the rich, rhythmic nature of endogenous hormone production. A promising trend in network neuroscience is to flip the cross-sectional model by tracking small samples of individuals over timescales of weeks, months, or years to provide insight into how biological, behavioral, and state-dependent factors influence intra- and inter-individual variability in the brain's intrinsic network organization[5–7]. Neuroimaging studies that densely sample the individual connectome are beginning to transform our understanding of the dynamics of human brain organization. However, these studies commonly overlook sex steroid hormones as a source of variability—a surprising omission given that sex hormones are powerful neuromodulators that display stable circadian, infradian, and circannual rhythms in nearly all mammalian species. In the present study, we illustrate robust, time-dependent interactions between the sex steroid hormones 17β-estradiol and progesterone and the functional network organization of the brain over a complete menstrual cycle, offering compelling evidence that sex hormones drive widespread patterns of connectivity in the human brain.

Converging evidence from rodent[1,2,8], non-human primate[9,10], and human neuroimaging studies[11–16] has established the widespread influence of 17β-estradiol and progesterone on regions of the mammalian brain that support higher level cognitive functions. Estradiol and progesterone signaling are critical components of cell survival and plasticity, exerting excitatory and inhibitory effects that are evident across multiple spatial and temporal scales[4,8]. The dense expression of estrogen and progesterone receptors (ER; PR) in cortical and subcortical tissue underscores the widespread nature of hormone action. For example, in non-human primates $\sim$50% of pyramidal neurons in prefrontal cortex (PFC) express ER[10] and estradiol regulates dendritic spine proliferation in this region[3]. In rodents, fluctuations in estradiol across the estrous cycle enhance spinogenesis in hippocampal CA1 neurons and progesterone inhibits this effect[1].

During an average human menstrual cycle, occurring every 25-32 days, women experience a $\sim$12-fold increase in estradiol and an $\sim$800-fold increase in progesterone. Despite this striking change in endocrine status, we lack a complete understanding of how the large-scale functional architecture of the human brain responds to rhythmic changes in sex hormone production across the menstrual cycle. Much of our understanding of cycle-dependent changes in brain structure[1,17] and function[18–20] comes from rodent studies, since the length of the human menstrual cycle (at least 5$\times$ longer than rodents') presents experimental hurdles that make longitudinal studies challenging. A common solution is to study women a few times throughout their cycle, targeting stages that roughly correspond to peak/trough hormone concentrations. Using this 'sparse-sampling' approach, studies

have examined resting-state connectivity in discrete stages of the cycle[13,14,21–23]; however, some of these findings are undermined by inconsistencies in cycle staging methods, lack of direct hormone assessments, or limitations in functional connectivity methods.

In this dense-sampling, deep-phenotyping study, we assessed brain-hormone interactions over 30 consecutive days representing a complete menstrual cycle. Our results reveal that intrinsic functional connectivity is influenced by hormone dynamics across the menstrual cycle at multiple spatiotemporal resolutions. Estradiol and progesterone conferred robust time-synchronous and time-lagged effects on the brain, demonstrating that intrinsic fluctuations in sex hormones drive changes in the functional network architecture of the human brain. Together, these findings provide insight into how brain networks reorganize across the human menstrual cycle and suggest that consideration of the hormonal milieu is critical for fully understanding the intrinsic dynamics of the human brain.

Results

A healthy, naturally-cycling female (author L.P.; age 23) underwent venipuncture and MRI scanning for 30 consecutive days. The full dataset consists of daily mood, diet, physical activity, and behavioral assessments, task-based and resting-state fMRI, structural MRI, and serum assessments of pituitary gonadotropins and ovarian sex hormones. Neuroimaging data, code, and daily behavioral assessments will be publicly accessible upon publication.

Endocrine assessments

Analysis of daily sex hormone (by liquid-chromatography mass-spectrometry; LC-MS) and gonadotropin (by chemiluminescent immunoassay) concentrations confirmed the expected rhythmic changes of a typical menstrual cycle, with a total cycle length of 27 days. Serum levels of estradiol and progesterone were lowest during menses (day 1-4) and peaked in late follicular (estradiol) and late luteal (progesterone) phases (**Fig. 1; Table 1**). Progesterone concentrations surpassed 5 ng/mL in the luteal phase, signaling an ovulatory cycle.

Time-synchronous associations between sex hormones and whole-brain functional connectivity

To begin, we tested the hypothesis that whole-brain functional connectivity at rest is associated with intrinsic fluctuations in estradiol and progesterone in a *time-synchronous* (i.e. day-by-day) fashion. Based on the enriched expression of ER in PFC[10], we predicted that the Default Mode, Frontoparietal Control, and Dorsal Attention Networks would be most sensitive to hormone fluctuations across the cycle. For each session, the brain was parcellated into 400 cortical regions from the Schaefer atlas[24] and 15 subcortical regions from the Harvard-Oxford atlas (**Fig. 2c**). A summary time-course was extracted from each parcel, data were temporally-filtered using a maximal overlap discrete wavelet transform (scales 3-6; $\sim$0.01–0.17 Hz), and 415 $\times$ 415 functional association matrices were constructed via magnitude-squared coherence (FDR-thresholded at $q < .05$; see **Online Methods** for a full description of preprocessing and connectivity estimation). Next, we specified edgewise

regression models, regressing coherence against estradiol and progesterone over the 30 days of the study. All data were Z-scored prior to analysis and models were thresholded against empirical null distributions generated through 10,000 iterations of nonparametric permutation testing. Results reported below survived a conservative threshold of $p < .001$.

We observed robust increases in coherence as a function of increasing estradiol across the brain (**Fig. 2a**). When summarizing across networks (computing the mean association strength across network nodes, where strength was defined per graph theory as the sum of positive and negative edge weights linked to each node, independently), components of the Temporal Parietal Network had the strongest positive associations on average, as well as the most variance (**Fig. 2d**). With the exception of Subcortical nodes, all networks demonstrated some level of significantly positive association strength (95% CIs not intersecting zero). We observed a paucity of edges showing inverse associations (connectivity decreasing while estradiol increased), with no networks demonstrating significantly negative association strengths on average (**Fig. 2d**). These findings suggest that edgewise functional connectivity is primarily characterized by increased coupling as estradiol rises over the course of the cycle.

Progesterone, by contrast, yielded a widespread pattern of inverse association across the brain, such that connectivity decreased as progesterone rose (**Fig. 2b**). Most networks (with the exception of the Salience/Ventral Attention and SomatoMotor Networks) still yielded some degree of significantly positive association over time; however, the general strength of negative associations was larger in magnitude and significantly nonzero across

all networks (**Fig. 2d**). Together, these results align with animal models suggesting excitatory and inhibitory roles for estradiol and progesterone, respectively, manifested here as predominant increases and decreases in functional connectivity across the cycle.

Time-lagged associations between estradiol and whole-brain functional connectivity

We then employed time-lagged methods from dynamical systems analysis to further elucidate the influence of hormonal fluctuations on intrinsic functional connectivity: specifically, vector autoregression (VAR), which supports more directed, causal inference than standard regression models. Here we chose to focus exclusively on estradiol for two reasons: 1) the highly-bimodal time-course of progesterone confers a considerably longer autocorrelative structure, requiring many more free parameters (i.e. higher-order models, ultimately affording fewer degrees of freedom); and 2) progesterone lacks an appreciable pattern of periodicity in its autocovariance with network timeseries, suggesting less relevance for time-lagged analysis over a single cycle. In contrast, estradiol has a much smoother time-course that is well-suited for temporal-evolution models such as VAR.

In short, VAR solves a simultaneous system of equations that predicts *current* states of the brain and estradiol from the *previous* states of each. We report results from second-order VAR models: thus, in order to predict connectivity or hormonal states on a given day of the experiment, we consider their values on both the previous day (hereafter referred to as 'lag 1') and two days prior (hereafter referred to as 'lag 2'). See **Online Methods** for an additional mathematical description. Ultimately, if brain variance over time is attributable

to previous states of estradiol, this suggests that temporal dynamics in connectivity may be *driven* (in part) by fluctuations in hormonal states. Vector autoregressive models were specified for each network edge; as before, all data were Z-scored and models were empirically thresholded against 10,000 iterations of nonparametric permutation testing. Surviving edges were significant at the $p < .001$ level.

When predicting edgewise connectivity states, a powerful disparity emerged between the brain's autoregressive effects and the effects of estradiol. We observed vast, whole-brain associations with prior hormonal states, both at lag 1 and lag 2 (**Fig. 3a**). Perhaps most immediately striking, the sign of these brain-hormone associations inverts between lags, such that it is predominantly positive at lag 1 and predominantly negative at lag 2—this holds for all networks when considering their nodal association strengths (**Fig. 3b**). We interpret this as a potential regulatory dance between brain states and hormones over the course of the cycle, with estradiol perhaps playing a role in maintaining both steady states (when estradiol is low) and transiently-high dynamics (when estradiol rises). No such pattern emerged in the brain's autoregressive effects, with sparse, low-magnitude, and predominantly negative associations at lag 1 and lag 2 (**Supplementary Fig. 1**). The flow of effect between estradiol and edgewise connectivity was partially unidirectional. Previous states of coherence predicted estradiol across a number of edges, intersecting all brain networks. This emerged at both lag 1 and lag 2; however, unlike the lagged effects of estradiol on coherence, association strengths were predominantly negative at both lags (**Supplementary Fig. 2**). Moreover—and importantly—none of the edges that

predicted estradiol were also significantly predicted *by* estradiol at either lag (i.e. there was no evidence of mutual modulation for any network edge).

Time-lagged associations between estradiol and functional network topologies

Given the findings above, we applied the same time-lagged framework to *topological states* of brain networks in order to better capture the directionality and extent of brain-hormone interactions at the network level. These states were quantified using common graph theory metrics: namely, the *participation coefficient* (an estimate of *between-network* integration) and *global efficiency* (an estimate of *within-network* integration). As before, all data were Z-scored prior to analysis, and model parameters/fit were compared against 10,000 iterations of nonparametric permutation testing. We focus on significant network-level effects below, but a full documentation of our findings is available in the **Supplementary Information**.

Estradiol and between-network participation

As expected, estradiol demonstrated significant autoregressive effects across all models. Previous states of estradiol also significantly predicted between-network integration across several intrinsic networks; however, overall model fit (variance accounted for, R^2, and root mean-squared error, $RMSE$) was at best marginal compared to empirical null distributions of these statistics. For example, in the Dorsal Attention Network (DAN; **Fig. 4a-b; Table 2**), estradiol was a significant predictor of between-network participation both at lag 1 ($b = -0.56, SE = 0.25, t = -2.27, p = .035$) and at lag 2 ($b = 0.53, SE = 0.24, t = 2.16, p = .042$). Overall fit for DAN participation, however, rested at the classical frequentist threshold

for significance, relative to empirical nulls ($R^2 = 0.32, p = .049$; $RMSE = 0.79, p = .050$). We observed a similar pattern of results for the Default Mode Network (DMN) and Limbic Network, where lagged states of estradiol significantly predicted cross-network participation, but model fit as a whole was low (see **Supplementary Table 1**). Interestingly, for all three of these networks, there were no significant autoregressive effects of brain states—previous states of network participation also did not predict estradiol, suggesting that modulation of network topology likely goes from hormones to brain, not the other way around.

The single exception to this trend was the Visual Network. Prediction of its between-network participation yielded a significant model fit ($R^2 = 0.37, p = .024; RMSE = 0.79, p = .044$). However, this was primarily driven by autoregressive effects of the network at lag 1 ($b = -0.39, SE = 0.17, t = -2.30, p = .027$) and lag 2 ($b = -0.43, SE = 0.17, t = -2.46, p = .024$); estradiol yielded a marginal (but nonsignificant) effect only at lag 2 ($b = 0.49, SE = 0.24, t = 2.01, p = .058$).

Estradiol and global efficiency

In contrast to between-network integration, estradiol was a strong predictor of within-network integration, both in terms of parameter estimates and overall fit. Here, the Default Mode Network provided the best-fitting model ($R^2 = 0.50, p = .003; RMSE = 0.70, p = .022$; **Fig. 5a-b**). As before, estradiol demonstrated significant autoregressive effects at lag 1 ($b = 1.15, SE = 0.19, t = 6.15, p < .0001$) and lag 2 ($b = -0.48, SE = 0.19, t = -2.50, p = .012$). When predicting DMN efficiency, previous states of estradiol

remained significant both at lag 1 ($b = 0.98, SE = 0.23, t = 3.37, p = .0003$) and at lag 2 ($b = -0.93, SE = 0.23, t = -4.00, p = .002$). Critically, these effects were purely directional: prior states of Default Mode efficiency did not predict estradiol, nor did they have significant autoregressive effects, supporting the conclusion that variance in topological network states (perhaps within-network integration, in particular) is primarily accounted for by estradiol—not the other way around (**Table 3**).

We observed a similar pattern of results in the Dorsal Attention Network ($R^2 = 0.37, p = .022; RMSE = 0.77, p = .023$; **Fig. 4c; Table 3**). Estradiol again demonstrated significant autoregressive effects at lag 1 ($b = 1.17, SE = 0.19, t = 6.30, p < .0001$) and lag 2 ($b = -0.48, SE = 0.19, t = -2.49, p = .011$), along with predicting DAN efficiency both at lag 1 ($b = 0.84, SE = 0.25, t = 3.35, p = .002$) and at lag 2 ($b = -0.67, SE = 0.16, t = -2.57, p = .017$). As above, Dorsal Attention efficiency had no significant effects on estradiol, nor were there significant autoregressive effects of the network on itself.

The Control and Temporal Parietal networks also yielded partial support for time-dependent modulation of efficiency by estradiol (Control $R^2 = 0.34, p = .039$; Temporal Parietal $R^2 = 0.36, p = .026$). The time-lagged effects of estradiol followed the trends observed above; however, the overall model fit (with respect to prediction error) was not significantly better than their empirical nulls (Control $RMSE = 0.83, p = .133$; Temporal Parietal $RMSE = 0.79, p = .057$). Estradiol did not explain a significant proportion of variance in efficiency for any other networks (see **Supplementary Table 2** for a complete summary of VAR models for global efficiency).

Discussion

In this dense-sampling, deep-phenotyping project, a naturally-cycling female underwent resting state fMRI and venipuncture for 30 consecutive days, capturing the dynamic endocrine changes that unfold over the course of a complete menstrual cycle. Time-synchronous analyses illustrate estradiol's widespread impact on cortical dynamics, spanning all but one of the networks in our parcellation. Time-lagged vector autoregressive models tested the temporal directionality of these effects, suggesting that intrinsic network dynamics are driven by recent states of estradiol, particularly with respect to within-network connectivity. Estradiol had the strongest predictive effects on the efficiency of Default Mode and Dorsal Attention Networks. In contrast to estradiol's proliferative effects, progesterone was primarily associated with reduced coherence across the whole brain. These results reveal the rhythmic nature of brain network reorganization across the human menstrual cycle.

The network neuroscience community has begun to probe functional networks over the timescale of weeks, months, and years to understand the extent to which brain networks vary between individuals or within an individual over time[5,6,25–27]. These studies indicate that functional networks are dominated by common organizational principles and stable individual features, especially in frontoparietal control regions[6,7,25,27]. An overlooked feature of these regions is the dense populations of estrogen and progesterone receptors, imparting exquisite sensitivity to major changes in sex hormone concentrations[11,12,15,16,28,29]. Our findings demonstrate significant effects of estradiol on functional network nodes

belonging to the DMN, DAN, and FCN that overlap with ER-rich regions of the brain, including medial/dorsal PFC[10,30]. This study merges the network neuroscience and endocrinology disciplines by demonstrating that higher-order processing systems are modulated by day-to-day changes in sex hormones over the timescale of one month.

Animal studies offer unambiguous evidence that sex steroid hormones shape the synaptic organization of the brain, particularly in regions that support higher order cognitive functions[1–4,8]. In rodents, estradiol increases fast-spiking interneuron excitability in deep cortical layers[31]. In nonhuman primates, whose reproductive cycle length is similar to humans, estradiol increases the number of synapses in PFC[3]. Recently, this body of work has also begun to uncover the functional significance of sinusoidal *changes* in estradiol. For example, estradiol's ability to promote PFC spinogenesis in ovariectomized animals occurs *only if* the hormone add-back regime mirrors the cyclic pattern of estradiol release typical of the macaque menstrual cycle[9,32]. Pairing estradiol with cyclic administration of progesterone blunts this increase in spine density[32]. In the hippocampus, progesterone has a similar inhibitory effect on dendritic spines, blocking the proliferative effects of estradiol 6 hours after administration[1]. Together, the preclinical literature suggests that progesterone antagonizes the largely proliferative effects of estradiol (for review, see Brinton and colleagues[33]). We observed a similar relationship, albeit at a different spatiotemporal resolution, with estradiol enhancing coherence across cortical networks and progesterone diminishing it. In sum, animal studies have identified estradiol's influence on regional brain organization at the microscopic scale. Here, we

show that estradiol and progesterone's influence is also evident at the mesoscopic scale of whole-brain activation, measured by spectral coherence, and macroscopic features of network topology.

Additional evidence from group-based or sparser-sampling neuroimaging studies provide further support that cycle stage and sex hormones impact resting state networks[13,14]. Arélin and colleagues[34] sampled an individual every 2-3 days across four cycles and found that progesterone was associated with increased connectivity between the hippocampus, dorsolateral PFC and the sensorimotor cortex, providing compelling evidence that inter-regional connectivity varies over the cycle. However, the sampling rate of this correlational study precluded the authors from capturing the neural effects of day-to-day changes in sex steroid hormones and from testing the temporal directionality of the effect with time-lagged models. Estradiol has both rapid, non-genomic effects and slower, genomic effects on the central nervous system. For example, over the rat estrous cycle, there is a dramatic 30% increase in hippocampal spine density within the 24-hour window in which estradiol concentrations peak. Here, we sought to capture both time-synchronous (rapid) and time-lagged (delayed) effects of sex steroid hormones, sampling every 24 hours for 30 consecutive days. In contrast to Arélin and colleagues, we observed robust, spatially-diffuse negative relationships between progesterone and coherence across the brain, while estradiol enhanced the global efficiency of discrete networks along with between-network integration. Our results illuminate how simultaneous, time-synchronous correlations and causal, time-lagged analysis reveal

unique aspects of where and how hormones exert their effect on the brain's intrinsic networks: time synchronous analyses illustrate estrogen and progesterone's widespread influence on cortical coupling, while vector autoregressive models allowed us to examine the temporal flow of effect in those relationships, showing that estradiol *drives* increased connectivity—particularly in DMN and DAN.

The following considerations could enhance the interpretation of these data. First, this study represents extensive neural phenotyping of a healthy participant with canonical hormone fluctuations over a reproductive cycle. To enrich our understanding of the relationship between sex hormones and brain function, examining network organization in a hormonally-suppressed female (i.e. an oral contraceptive user) would serve as a valuable comparison. Oral hormonal contraceptives suppress the production of ovarian hormones: if dynamic changes in estradiol are indeed *causing* increases in resting connectivity, we expect hormonally-suppressed individuals to show blunted functional brain network dynamics over time. Given the widespread use of oral hormonal contraceptives (100 million users worldwide), it is critical to determine whether sweeping changes to an individual's endocrine state impacts brain states and whether this, in turn, has any bearing on cognition.

Second, in normally-cycling individuals, sex hormones function as proportionally-coupled *nonlinear* oscillators[35]. Within-person cycle variability is almost as large as between-person cycle variability, which hints that there are highly-complex hormonal interactions within this regulatory system[35,36]. The VAR models we have

explored reveal linear dependencies between brain states and hormones, but other dynamical systems methods (e.g. coupled latent differential equations) may offer more biophysical validity[35]. Unfortunately, the current sample of only one individual across one complete cycle precludes robust estimation of such a model. Future studies should enroll a larger sample of women to assess whether individual differences in hormone dynamics drive network changes.

Third, while coherence is theoretically robust to timing differences in the hemodynamic response function, hormones can affect the vascular system[37]. Therefore, changes in coherence may be due to vascular artifacts that affect the hemodynamic response in fMRI, rather than being *neurally*-relevant. Future investigations exploring the assumptions of hemodynamics in relation to sex steroid hormone concentrations will add clarity as to how the vascular system's response to hormones might influence large-scale brain function.

Fourth, these findings contribute to an emerging body of work on estradiol's ability to enhance the efficiency of PFC-based cortical circuits. In young women performing a working memory task, PFC activity is exaggerated under low estradiol conditions and reduced under high estradiol conditions[12]. The same pattern is observed decades later in life: as estradiol production decreases over the menopausal transition, working memory-related PFC activity becomes more exaggerated, despite no difference in working memory performance[15]. Here, we show that day-to-day changes in estradiol drive the global efficiency of functional networks, with the most pronounced effects in networks with

major hubs in the PFC. Together, these findings suggest that estradiol generates a neurally efficient PFC response at rest and while engaging in a cognitive task. The mechanism by which this occurs may be through enhancing dopamine synthesis and release[38]: the PFC is innervated by midbrain dopaminergic neurons that form the mesocortical dopamine track[39]. Decades of evidence have established that dopamine signaling enhances the signal-to-noise ratio of PFC pyramidal neurons[40] and drives cortical efficiency[41–44]. More recently it was discovered that estradiol enhances dopamine synthesis, release, and turnover and modifies the basal firing rate of dopaminergic neurons[45–47], a plausible neurobiological mechanism by which alterations in estradiol could impact cortical efficiency. Future multimodal neuroimaging studies in humans can clarify the link between estradiol's ability to stimulate dopamine release and the hormone's ability to drive cortical efficiency within PFC circuits.

Using dense-sampling approaches to probe brain-hormone interactions could reveal organizational principles of the functional connectome previously unknown, transforming our understanding of how hormones influence brain states. Human studies implicate sex steroids in the regulation of brain structure and function, particularly within ER-rich regions like the PFC and hippocampus[11,12,15,16,28,29,48–50], yet the neuroendocrine basis of the brain's network organization remains understudied. A network neuroscience approach allows us to understand how hormones modulate the integration of functional brain networks that span the entire cortical surface and subcortex, as opposed to examining discrete brain regions in isolation. Using this approach, we show that estradiol is associated

with increased coherence across broad swaths of cortex. At the network level, estradiol enhances the efficiency of most functional networks (with robust effects in DAN and DMN) and, to a lesser extent, increases between-network participation. Moving forward, this network neuroscience approach can be applied to brain imaging studies of other major neuroendocrine transitions, such as pubertal development and reproductive aging (e.g. menopause).

An overarching goal of network neuroscience is to understand how coordinated activity within and between functional brain networks supports cognition. Increased global efficiency is thought to optimize a cognitive workspace[51], while between-network connectivity may be integral for integrating top-down signals from multiple higher-order control hubs[52]. The dynamic reconfiguration of functional brain networks is implicated in performance across cognitive domains, including motor learning[53,54], cognitive control[55], and memory[56]. Our results demonstrate that within- and between-network connectivity of these large-scale networks at rest are hormonally regulated across the human menstrual cycle. Future studies should consider whether these network changes confer advantages to domain-general or domain-specific cognitive performance. Further, planned analyses from this dataset will incorporate task-based fMRI to determine whether the brain's network architecture is hormonally regulated across the cycle when engaging in a cognitive task, or in the dynamic reconfiguration that occurs when transitioning from rest to task.

The emerging field of clinical network neuroscience also seeks to understand how large-scale brain networks differ between healthy and patient populations[57,58].

Disruptions in functional brain networks are implicated in a number of neurodegenerative and neuropsychiatric disorders. For example, intrinsic connectivity abnormalities in the DMN are evident in major depressive disorder[59] and Alzheimer's disease[60]. Notably, these conditions have a sex-skewed disease prevalence: women are at twice the risk for depression and make up two-thirds of the Alzheimer's disease patient population[61]. Here, we show that global efficiency in the DMN and DAN are hormonally regulated, with estradiol driving increases in within-network integration. A long history of clinical evidence further implicates sex hormones in the development of mood disorders[62,63]. Throughout the lifecourse, changes in women's reproductive status have been associated with increased risk for depression[64–67]. For example, the incidence of major depression increases with pubertal onset in females[68], chronic use of hormonal contraceptives[69], the postpartum period[70], and perimenopause[71]. Moving forward, a network neuroscience approach could identify the large-scale network disturbances that underlie, or predict, the emergence of disease symptomology. Incorporating sex-dependent variables (such as endocrine status) into clinical network neuroscience models may be essential for identifying individuals at risk of disease. This may be particularly true during periods of profound neuroendocrine change (e.g. puberty, pregnancy, menopause, and use of hormone-based medications, reviewed by Taylor and colleagues[72]) given that these hormonal transitions are associated with a heightened risk for mood disorders.

In sum, endogenous hormone fluctuations over the reproductive cycle have a robust impact on the intrinsic network properties of the human brain. Despite over 20 years of

evidence from rodent, nonhuman primate, and human studies demonstrating the tightly-coupled relationship between our endocrine and nervous systems, the field of network neuroscience has largely overlooked how endocrine factors shape the brain. The dynamic endocrine changes that unfold over the menstrual cycle are a natural feature of half of the world's population. Understanding how these changes in sex hormones influence the large-scale functional architecture of the human brain is imperative for our basic understanding of the brain and for women's health.

End Notes

Acknowledgements. This work was supported by the Brain and Behavior Research Foundation (EGJ), the California Nanosystems Institute (EGJ), the Institute for Collaborative Biotechnologies through grant W911NF-19-D-0001 from the U.S. Army Research Office (MBM), and the Rutherford B. Fett Fund (SG). Thanks to Mario Mendoza for phlebotomy and MRI assistance. We would also like to thank Courtney Kenyon, Maggie Hayes, and Morgan Fitzgerald for assistance with data collection.

Author contributions. The overall study was conceived by L.P., C.M.T., and E.G.J.; L.P., T.S., E.L., C.M.T., S.Y., and E.G.J. performed the experiments; data analysis strategy was conceived by T.S. and L.P. and implemented by T.S.; L.P., T.S., and E.G.J. wrote the manuscript; E.L., C.M.T., S.Y., M.B.M., and S.T.G. edited the manuscript.

Data/code availability. MRI data, code, and daily behavioral assessments will be publicly accessible upon publication.

Conflict of interest. The authors declare no competing financial interests.

Online Methods

Participants

The participant (author L.P.) was a right-handed Caucasian female, aged 23 years for duration of the study. The participant had no history of neuropsychiatric diagnosis, endocrine disorders, or prior head trauma. She had a history of regular menstrual cycles (no missed periods, cycle occurring every 26-28 days) and had not taken hormone-based medication in the prior 12 months. The participant gave written informed consent and the study was approved by the University of California, Santa Barbara Human Subjects Committee.

Study design

The participant underwent daily testing for 30 consecutive days, with the first test session determined independently of cycle stage for maximal blindness to hormone status. The participant began each test session with a daily questionnaire (see **Behavioral assessment**), followed by an immersive reality spatial navigation task (not reported here) (**Fig. 6**). Time-locked collection of serum and whole blood started each day at 10:00am, when the participant gave a blood sample. Endocrine samples were collected, at minimum, after two hours of no food or drink consumption (excluding water). The participant refrained from consuming caffeinated beverages before each test session. The MRI session lasted one hour and consisted of structural and functional MRI sequences.

Behavioral assessments

To monitor state-dependent mood and lifestyle measures over the cycle, the following scales (adapted to reflect the past 24 hours) were administered each morning: Perceived Stress Scale (PSS)[73], Pittsburgh Sleep Quality Index (PSQI)[74], State-Trait Anxiety Inventory for Adults (STAI)[75], Profile of Mood States (POMS)[76], and the Sexual Desire Inventory-2 (SDI-2)[77]. We observed very few significant relationships between hormone and state-dependent measures following an FDR-correction for multiple comparisons ($q < .05$)—and critically, none of these state-dependent factors were associated with estradiol (**Fig. 7a**). The participant had moderate levels of anxiety as determined by STAI reference ranges; however, all other measures fell within the 'normal' standard range (**Fig. 7b**).

Endocrine procedures

A licensed phlebotomist inserted a saline-lock intravenous line into the dominant or non-dominant hand or forearm daily to evaluate hypothalamic-pituitary-gonadal axis hormones, including serum levels of gonadal hormones (17β-estradiol, progesterone and testosterone) and the pituitary gonadotropins luteinizing hormone (LH) and follicle stimulating hormone (FSH). One 10cc mL blood sample was collected in a vacutainer SST (BD Diagnostic Systems) each session. The sample clotted at room temperature for 45 min until centrifugation (2,000 $\times g$ for 10 minutes) and were then aliquoted into three 1 ml microtubes. Serum samples were stored at -20° C until assayed. Serum concentrations were determined via liquid chromatography-mass spectrometry (for all steroid hormones)

and immunoassay (for all gonadotropins) at the Brigham and Women's Hospital Research Assay Core. Assay sensitivities, dynamic range, and intra-assay coefficients of variation (respectively) were as follows: estradiol, 1 pg/mL, 1–500 pg/mL, $< 5\%$ relative standard deviation (RSD); progesterone, 0.05 ng/mL, 0.05–10 ng/mL, 9.33% RSD; testosterone, 1.0 ng/dL, 1–2000 ng/dL, $<$ 4% RSD; FSH and LH levels were determined via chemiluminescent assay (Beckman Coulter). The assay sensitivity, dynamic range, and the intra-assay coefficient of variation were as follows: FSH, 0.2 mIU/mL, 0.2–200 mIU/mL, 3.1–4.3%; LH, 0.2 mIU/mL, 0.2–250 mIU/mL, 4.3–6.4%.

fMRI acquisition and preprocessing

The participant underwent a daily magnetic resonance imaging scan on a Siemens 3T Prisma scanner equipped with a 64-channel phased-array head coil. First, high-resolution anatomical scans were acquired using a T_1-weighted magnetization prepared rapid gradient echo (MPRAGE) sequence (TR = 2500 ms, TE = 2.31 ms, TI = 934 ms, flip angle = 7°; 0.8 mm thickness) followed by a gradient echo fieldmap (TR = 758 ms, TE_1 = 4.92 ms, TE_2 = 7.38 ms, flip angle = 60°). Next, the participant completed a 10-minute resting-state fMRI scan using a T_2^*-weighted multiband echo-planar imaging (EPI) sequence sensitive to the blood oxygenation level-dependent (BOLD) contrast (TR = 720 ms, TE = 37 ms, flip angle = 56°, multiband factor = 8; 72 oblique slices, voxel size = 2 mm^3). In an effort to minimize motion, the head was secured with a custom, 3D-printed foam head case (https://caseforge.co/) (days 8-30). Overall motion (mean framewise displacement) was negligible (**Supplementary Fig. 3**), with fewer than 130 microns of

motion on average each day. Importantly, mean framewise displacement was also not correlated with estradiol concentrations (Spearman $r = -0.06, p = .758$).

Initial preprocessing was performed using the Statistical Parametric Mapping 12 software (SPM12, Wellcome Trust Centre for Neuroimaging, London) in Matlab. Functional data were realigned and unwarped to correct for head motion and the mean motion-corrected image was coregistered to the high-resolution anatomical image. All scans were then registered to a subject-specific anatomical template created using Advanced Normalization Tools (ANTs) multivariate template construction (**Supplementary Fig. 4**). A 5 mm full-width at half-maximum (FWHM) isotropic Gaussian kernel was subsequently applied to smooth the functional data. Further preparation for resting-state functional connectivity was implemented using in-house Matlab scripts. Global signal scaling (median = 1,000) was applied to account for fluctuations in signal intensity across space and time, and voxelwise timeseries were linearly detrended. Residual BOLD signal from each voxel was extracted after removing the effects of head motion and five physiological noise components (CSF + white matter signal). Motion was modeled based on the Friston-24 approach, using a Volterra expansion of translational/rotational motion parameters, accounting for autoregressive and nonlinear effects of head motion on the BOLD signal[78]. All nuisance regressors were detrended to match the BOLD timeseries.

Functional connectivity estimation

Functional network nodes were defined based on a 400-region cortical parcellation[24] and 15 regions from the Harvard-Oxford subcortical atlas (`http://www.fmrib.ox.ac.uk/fsl/`). For each day, a summary timecourse was extracted per node by taking the first eigenvariate across functional volumes[79]. These regional timeseries were then decomposed into several frequency bands using a maximal overlap discrete wavelet transform. Low-frequency fluctuations in wavelets 3–6 ($\sim$0.01–0.17 Hz) were selected for subsequent connectivity analyses[80]. Finally, we estimated the spectral association between regional timeseries using magnitude-squared coherence: this yielded a 415×415 functional association matrix each day, whose elements indicated the strength of functional connectivity between all pairs of nodes (FDR-thresholded at $q < .05$).

Statistical analysis

First, we assessed time-synchronous variation in functional connectivity associated with estradiol and progesterone through a standardized regression analysis. Data were Z-transformed and edgewise coherence was regressed against hormonal timeseries to capture day-by-day variation in connectivity relative to hormonal fluctuations. For each model, we computed robust empirical null distributions of test-statistics via 10,000 iterations of nonparametric permutation testing—while this process has been shown to adequately approximate false positive rates of 5%[81], we elected to report only those edges surviving a conservative threshold of $p < .001$ to avoid over-interpretation of whole-brain effects.

Next, we sought to capture *causal* linear dependencies between estradiol and network connectivity over time using vector autoregressive (VAR) models. A given VAR model takes a set of variables at time, t, and simultaneously regresses them against previous (time-lagged) states of themselves and each other. For consistency, we only considered second-order VAR models, given a fairly reliable first zero-crossing of brain/hormone autocovariance functions at lag two. Fit parameters for each VAR therefore reflect the following general form:

$$Brain_t = b_{1,0} + b_{1,1}Brain_{t-1} + b_{1,2}Estradiol_{t-1} + b_{1,3}Brain_{t-2} + b_{1,4}Estradiol_{t-2} + e_t$$

$$Estradiol_t = b_{2,0} + b_{2,1}Brain_{t-1} + b_{2,2}Estradiol_{t-1} + b_{2,3}Brain_{t-2} + b_{2,4}Estradiol_{t-2} + e_t \quad (1)$$

With respect to brain states, we modeled both edgewise coherence and factors related to macroscale network topologies. Specifically, we computed measures of *between-network* integration (the participation coefficient; i.e. the average extent to which network nodes are communicating with other networks over time) and *within-network* integration (global efficiency, quantifying the ostensible ease of information transfer across nodes inside a given network). Regardless of brain measure, each VAR was estimated similarly to the time-synchronous analyses described above: data were Z-scored, models were fit, and all effects were empirically-thresholded against 10,000 iterations of nonparametric permutation testing.

Finally, for each set of edgewise models (time-synchronous and time-lagged), we attempted to disentangle both the general *direction* of hormone-related associations and

whether certain networks were more or less *susceptible* to hormonal fluctuations. Toward that end, we estimated *nodal association strengths* per graph theory's treatment of signed, weighted networks—that is, positive and negative association strengths were computed independently for each node by summing the positive and negative edges linked to them (after empirical thresholding), respectively. We then simply assessed mean association strengths across the various networks in our parcellation.

Here, networks were defined by grouping the subnetworks of the 17-network Schaefer parcellation, such that (for example), the A, B, and C components of the Default Mode Network were treated as one network. We chose this due to the presence of a unique Temporal Parietal Network in the 17-network partition, which is otherwise subsumed by several other networks (Default Mode, Ventral Attention, and SomatoMotor) in the 7-network partition. The subcortical nodes of the Harvard-Oxford atlas were also treated as their own network, yielding a total of nine networks. These definitions were subsequently used for computation of participation coefficients and global efficiencies in network-level VAR models.

Brain data visualization

Statistical maps of edgewise coherence v. hormones were visualized using the Surf Ice software (`https://www.nitrc.org/projects/surfice/`).

References

[1] Woolley, C. S. & McEwen, B. S. Roles of estradiol and progesterone in regulation of hippocampal dendritic spine density during the estrous cycle in the rat. *J. Comp. Neurol.* **336**, 293–306 (1993).

[2] Frick, K. M., Kim, J., Tuscher, J. J. & Fortress, A. M. Sex steroid hormones matter for learning and memory: Estrogenic regulation of hippocampal function in male and female rodents. *Learn. Mem.* **22**, 472–493 (2015).

[3] Hara, Y., Waters, E. M., McEwen, B. S. & Morrison, J. H. Estrogen effects on cognitive and synaptic health over the lifecourse. *Physiol. Rev.* **95**, 785–807 (2015).

[4] Galea, L. A. M., Frick, K. M., Hampson, E., Sohrabji, F. & Choleris, E. Why estrogens matter for behavior and brain health. *Neurosci. Biobehav. Rev.* **76**, 363–379 (2017).

[5] Poldrack, R. A. *et al.* Long-term neural and physiological phenotyping of a single human. *Nat. Commun.* **6**, 8885 (2015).

[6] Gordon, E. M. *et al.* Precision functional fapping of individual human brains. *Neuron* **95**, 791–807 (2017).

[7] Gratton, C. *et al.* Functional brain networks are dominated by stable group and individual factors, not cognitive or daily variation. *Neuron* **98**, 439–452 (2018).

[8] Frick, K. M., Kim, J. & Koss, W. A. Estradiol and hippocampal memory in female and male rodents. *Curr. Opin. Behav. Sci.* **23**, 65–74 (2018).

[9] Hao, J. *et al.* Estrogen alters spine number and morphology in prefrontal cortex of aged female rhesus monkeys. *J. Neurosci.* **26**, 2571–2578 (2006).

[10] Wang, A. C. J., Hara, Y., Janssen, W. G. M., Rapp, P. R. & Morrison, J. H. Synaptic estrogen receptor-alpha levels in prefrontal cortex in female rhesus monkeys and their correlation with cognitive performance. *J. Neurosci.* **30**, 12770–12776 (2010).

[11] Berman, K. F. *et al.* Modulation of cognition-specific cortical activity by gonadal steroids: a positron-emission tomography study in women. *Proc. Natl. Acad. Sci. U.S.A.* **94**, 8836–8841 (1997).

[12] Jacobs, E. & D'Esposito, M. Estrogen shapes dopamine-dependent cognitive processes: Implications for women's health. *J. Neurosci.* **31**, 5286–5293 (2011).

[13] Petersen, N., Kilpatrick, L. A., Goharzad, A. & Cahill, L. Oral contraceptive pill use and menstrual cycle phase are associated with altered resting state functional connectivity. *Neuroimage* **90**, 24–32 (2014).

[14] Lisofsky, N. *et al.* Hippocampal volume and functional connectivity changes during the female menstrual cycle. *Neuroimage* **118**, 154–162 (2015).

[15] Jacobs, E. G. *et al.* Reorganization of functional networks in verbal working memory circuitry in early midlife: The impact of sex and menopausal status. *Cereb. Cortex* **27**, 2857–2870 (2016).

[16] Jacobs, E. G. *et al.* Impact of sex and menopausal status on episodic memory circuitry in early midlife. *J. Neurosci.* **36**, 10163–10173 (2016).

[17] Sheppard, P. A. S., Choleris, E. & Galea, L. A. M. Structural plasticity of the hippocampus in response to estrogens in female rodents. *Mol. Brain* **12**, 22 (2019).

[18] Warren, S. G. & Juraska, J. M. Spatial and nonspatial learning across the rat estrous cycle. *Behav. Neurosci.* **111**, 259–266 (1997).

[19] Hampson, E., Levy-Cooperman, N. & Korman, J. M. Estradiol and mental rotation: Relation to dimensionality, difficulty, or angular disparity? *Horm. Behav.* **65**, 238–248 (2014).

[20] Kim, J. & Frick, K. M. Distinct effects of estrogen receptor antagonism on object recognition and spatial memory consolidation in ovariectomized mice. *Psychoneuroendocrinology* **85**, 110–114 (2017).

[21] Hjelmervik, H., Hausmann, M., Osnes, B., Westerhausen, R. & Specht, K. Resting states are resting traits—an fmri study of sex differences and menstrual cycle effects in resting state cognitive control networks. *PLoS One* **9**, e103492 (2014).

[22] De Bondt, T. *et al.* Stability of resting state networks in the female brain during hormonal changes and their relation to premenstrual symptoms. *Brain Res.* **1624**, 275–285 (2015).

[23] Syan, S. K. *et al.* Influence of endogenous estradiol, progesterone, allopregnanolone, and dehydroepiandrosterone sulfate on brain resting state functional connectivity across the menstrual cycle. *Fertil. Steril.* **107**, 1246–1255 (2017).

[24] Schaefer, A. *et al.* Local-global parcellation of the human cerebral cortex from intrinsic functional connectivity mri. *Cereb. Cortex* **28**, 3095–3114 (2018).

[25] Finn, E. S. *et al.* Functional connectome fingerprinting: Identifying individuals using patterns of brain connectivity. *Nat. Neurosci.* **18**, 1664–1671 (2015).

[26] Betzel, R. F. *et al.* The community structure of functional brain networks exhibits scale-specific patterns of inter- and intra-subject variability. *Neuroimage* (2019).

[27] Horien, C., Shen, X., Scheinost, D. & Constable, R. T. The individual functional connectome is unique and stable over months to years. *Neuroimage* **189**, 676–687 (2019).

[28] Hampson, E. & Morley, E. E. Estradiol concentrations and working memory performance in women of reproductive age. *Psychoneuroendocrinology* **38**, 2897–2904 (2013).

[29] Shanmugan, S. & Epperson, C. N. Estrogen and the prefrontal cortex: towards a new understanding of estrogen's effects on executive functions in the menopause transition. *Hum. Brain. Mapp.* **35**, 847–865 (2014).

[30] Yeo, B. T. T. *et al.* The organization of the human cerebral cortex estimated by intrinsic functional connectivity. *J. Neurophysiol.* **106**, 1125–1165 (2011).

[31] Clemens, A. M. *et al.* Estrus-cycle regulation of cortical inhibition. *Curr. Biol.* **29**, 605–615 (2019).

[32] Ohm, D. T. *et al.* Clinically relevant hormone treatments fail to induce spinogenesis in prefrontal cortex of aged female rhesus monkeys. *J. Neurosci.* **32**, 11700–11705 (2012).

[33] Brinton, R. D. *et al.* Progesterone receptors: form and function in brain. *Front. Neuroendocrinol.* **29**, 313–339 (2008).

[34] Arelin, K. *et al.* Progesterone mediates brain functional connectivity changes during the menstrual cycle-a pilot resting state mri study. *Front. Neurosci.* **9**, 44 (2015).

[35] Boker, S. M., Neale, M. C. & Klump, K. L. *A differential equations model for the ovarian hormone cycle.*, 369–391 (Guilford Press, New York, 2014).

[36] Fehring, R. J., Schneider, M. & Raviele, K. Variability in the phases of the menstrual cycle. *J. Obstet. Gynecol. Neonatal. Nurs.* **35**, 376–384 (2006).

[37] Krause, D. N., Duckles, S. P. & Pelligrino, D. A. Influence of sex steroid hormones on cerebrovascular function. *J. Appl. Physiol.* **101**, 1252–1261 (2006).

[38] Creutz, L. M. & Kritzer, M. F. Estrogen receptor-beta immunoreactivity in the midbrain of adult rats: regional, subregional, and cellular localization in the a10, a9, and a8 dopamine cell groups. *J. Comp. Neurol.* **446**, 288–300 (2002).

[39] Kritzer, M. F. & Creutz, L. M. Region and sex differences in constituent dopamine neurons and immunoreactivity for intracellular estrogen and androgen receptors in mesocortical projections in rats. *J. Neurosci.* **28**, 9525–9535 (2008).

[40] Williams, G. V. & Goldman-Rakic, P. S. Modulation of memory fields by dopamine d1 receptors in prefrontal cortex. *Nature* **376**, 572–575 (1995).

[41] Cai, J. X. & Arnsten, A. F. Dose-dependent effects of the dopamine d1 receptor agonists a77636 or skf81297 on spatial working memory in aged monkeys. *J. Pharmacol. Exp. Ther.* **283**, 183–189 (1997).

[42] Granon, S. *et al.* Enhanced and impaired attentional performance after infusion of d1 dopaminergic receptor agents into rat prefrontal cortex. *J. Neurosci.* **20**, 1208–1215 (2000).

[43] Gibbs, S. E. B. & D'Esposito, M. Individual capacity differences predict working memory performance and prefrontal activity following dopamine receptor stimulation. *Cogn. Affect. Behav. Neurosci.* **5**, 212–221 (2005).

[44] Vijayraghavan, S., Wang, M., Birnbaum, S. G., Williams, G. V. & Arnsten, A. F. T. Inverted-u dopamine d1 receptor actions on prefrontal neurons engaged in working memory. *Nat. Neurosci.* **10**, 376–384 (2007).

[45] Thompson, T. L. & Moss, R. L. Estrogen regulation of dopamine release in the nucleus accumbens: genomic- and nongenomic-mediated effects. *J. Neurochem.* **62**, 1750–1756 (1994).

[46] Pasqualini, C., Olivier, V., Guibert, B., Frain, O. & Leviel, V. Acute stimulatory effect of estradiol on striatal dopamine synthesis. *J. Neurochem.* **65**, 1651–1657 (1995).

[47] Becker, J. B. Estrogen rapidly potentiates amphetamine-induced striatal dopamine release and rotational behavior during microdialysis. *Neurosci. Lett.* **118**, 169–171 (1990).

[48] Jacobs, E. G. *et al.* 17beta-estradiol differentially regulates stress circuitry activity in healthy and depressed women. *Neuropsychopharmacology* **40**, 566–576 (2015).

[49] Girard, R. *et al.* Hormone therapy at early post-menopause increases cognitive control-related prefrontal activity. *Sci. Rep.* **7**, 44917 (2017).

[50] Zeydan, B. *et al.* Association of bilateral salpingo-oophorectomy before menopause onset with medial temporal lobe neurodegeneration. *JAMA Neurol.* **76**, 95–100 (2019).

[51] Bullmore, E. T. & Bassett, D. S. Brain graphs: graphical models of the human brain connectome. *Annu. Rev. Clin. Psychol.* **7**, 113–140 (2011).

[52] Gratton, C., Sun, H. & Petersen, S. E. Control networks and hubs. *Psychophysiology* **55** (2018).

[53] Bassett, D. S. *et al.* Dynamic reconfiguration of human brain networks during learning. *Proc. Natl. Acad. Sci. U.S.A.* **108**, 7641–7646 (2011).

[54] Mattar, M. G. *et al.* Predicting future learning from baseline network architecture. *Neuroimage* **172**, 107–117 (2018).

[55] Seeley, W. W. *et al.* Dissociable intrinsic connectivity networks for salience processing and executive control. *J. Neurosci.* **27**, 2349–2356 (2007).

[56] Fornito, A., Harrison, B. J., Zalesky, A. & Simons, J. S. Competitive and cooperative dynamics of large-scale brain functional networks supporting recollection. *Proc. Natl. Acad. Sci. U.S.A.* **109**, 12788–12793 (2012).

[57] Fox, M. D. & Greicius, M. Clinical applications of resting state functional connectivity. *Front. Syst. Neurosci.* **4**, 19 (2010).

[58] Hallquist, M. N. & Hillary, F. G. Graph theory approaches to functional network organization in brain disorders: A critique for a brave new small-world. *Netw. Neurosci.* **3**, 1–26 (2019).

[59] Greicius, M. D. *et al.* Resting-state functional connectivity in major depression: Abnormally increased contributions from subgenual cingulate cortex and thalamus. *Biol. Psychiatry* **62**, 429–437 (2007).

[60] Buckner, R. L. *et al.* Cortical hubs revealed by intrinsic functional connectivity: mapping, assessment of stability, and relation to alzheimer's disease. *J. Neurosci.* **29**, 1860–1873 (2009).

[61] Nebel, R. A. *et al.* Understanding the impact of sex and gender in alzheimer's disease: A call to action. *Alzheimers Dement.* **14**, 1171–1183 (2018).

[62] Plotsky, P. M., Owens, M. J. & Nemeroff, C. B. Psychoneuroendocrinology of depression: hypothalamic-pituitary-adrenal axis. *Psychiatr. Clin. North. Am.* **21**, 293–307 (1998).

[63] Young, E. A. & Korszun, A. The hypothalamic-pituitary-gonadal axis in mood disorders. *Endocrinol. Metab. Clin. North. Am.* **31**, 63–78 (2002).

[64] Payne, J. L. The role of estrogen in mood disorders in women. *Int. Rev. Psychiatry* **15**, 280–290 (2003).

[65] Roca, C. A. *et al.* Differential menstrual cycle regulation of hypothalamic-pituitary-adrenal axis in women with premenstrual syndrome and controls. *J. Clin. Endocrinol. Metab.* **88**, 3057–3063 (2003).

[66] Rubinow, D. R. & Schmidt, P. J. Gonadal steroid regulation of mood: the lessons of premenstrual syndrome. *Front. Neuroendocrinol.* **27**, 210–216 (2006).

[67] Freeman, E. W., Sammel, M. D., Boorman, D. W. & Zhang, R. Longitudinal pattern of depressive symptoms around natural menopause. *JAMA Psychiatry* **71**, 36–43 (2014).

[68] Angold, A. & Costello, E. J. Puberty and depression. *Child Adolesc. Psychiatr. Clin. N. Am.* **15**, 919–937 (2006).

[69] Young, E. A. *et al.* Influences of hormone-based contraception on depressive symptoms in premenopausal women with major depression. *Psychoneuroendocrinology* **32**, 843–853 (2007).

[70] Bloch, M. *et al.* Effects of gonadal steroids in women with a history of postpartum depression. *Am. J. Psychiatry* **157**, 924–930 (2000).

[71] Schmidt, P. J. & Rubinow, D. R. Sex hormones and mood in the perimenopause. *Ann. N. Y. Acad. Sci.* **1179**, 70–85 (2009).

[72] Taylor, C. M., Pritschet, L., Yu, S. & Jacobs, E. G. Applying a women's health lens to the study of the aging brain. *Front. Hum. Neurosci.* **13**, 224 (2019).

[73] Cohen, S., Kamarck, T. & Mermelstein, R. A global measure of perceived stress. *J. Health. Soc. Behav.* **24**, 385–396 (1983).

[74] Buysse, D. J., Reynolds, C. F. r., Monk, T. H., Berman, S. R. & Kupfer, D. J. The pittsburgh sleep quality index: a new instrument for psychiatric practice and research. *Psychiatry Res.* **28**, 193–213 (1989).

[75] Spielberger, C. D. & Vagg, P. R. Psychometric properties of the stai: a reply to ramanaiah, franzen, and schill. *J. Pers. Assess.* **48**, 95–97 (1984).

[76] Pollock, V., Cho, D. W., Reker, D. & Volavka, J. Profile of mood states: the factors and their physiological correlates. *J. Nerv. Ment. Dis.* **167**, 612–614 (1979).

[77] Spector, I. P., Carey, M. P. & Steinberg, L. The sexual desire inventory: development, factor structure, and evidence of reliability. *J. Sex. Marital. Ther.* **22**, 175–190 (1996).

[78] Friston, K. J., Williams, S., Howard, R., Frackowiak, R. S. & Turner, R. Movement-related effects in fmri time-series. *Magn. Reson. Med.* **35**, 346–355 (1996).

[79] Bedenbender, J. *et al.* Functional connectivity analyses in imaging genetics: considerations on methods and data interpretation. *PLoS One* **6**, e26354 (2011).

[80] Patel, A. X. & Bullmore, E. T. A wavelet-based estimator of the degrees of freedom in denoised fmri time series for probabilistic testing of functional connectivity and brain graphs. *Neuroimage* **142**, 14–26 (2016).

[81] Eklund, A., Nichols, T. E. & Knutsson, H. Cluster failure: Why fmri inferences for spatial extent have inflated false-positive rates. *Proc. Natl. Acad. Sci. U.S.A.* **113**, 7900–7905 (2016).

List of Tables

Table 1. Gonadal and pituitary hormones by cycle stage.

	Follicular	**Ovulatory**	**Luteal**
	Mean (SD) *standard range*	Mean (SD) *standard range*	Mean (SD) *standard range*
Estradiol (pg/mL)	37.9 (15.9) *12.5-166.0*	185.3 (59.0) *85.8-498.0*	85.4 (26.4) *43.8-210.0*
Progesterone (ng/mL)	0.2 (0.2) *0.1-0.9*	0.2 (.2) *0.1-120*	9.5 (4.8) *1.8-23.9*
LH (mIU/mL)	5.9 (0.7) *2.4-12.6*	21.7 (16.4) *14.0-95.6*	5.5 (2.0) *1.0-11.4*
FSH (mIU/mL)	6.5 (1.2) *3.5-12.5*	8.1 (3.6) *4.7-21.5*	4.8 (1.3) *1.7-7.7*

Note. Standard reference ranges based on aggregate data from Labcorb (https://www.labcorp.com/)

Table 2. Vector autoregressive model for cross-network participation.

Network	Outcome	Predictor	Estimate	*SE*	*T* (*p*)
Dorsal Attention	Participation	Constant	0.08	0.16	0.49 (.099)
		DAN_{t-1}	0.15	0.18	0.84 (.405)
		$Estradiol_{t-1}$	**-0.56**	**0.25**	**-2.27 (.035)**
		DAN_{t-2}	-0.29	0.17	-1.71 (.093)
		$Estradiol_{t-2}$	**0.53**	**0.24**	**2.16 (.042)**
			R^2 = 0.32 (*p* = .049); *RMSE* = 0.79 (*p* = .050)		
	Estradiol	Constant	6.88×10^{-5}	0.12	0.001 (.998)
		DAN_{t-1}	0.06	0.14	0.47 (.627)
		$Estradiol_{t-1}$	**1.12**	**0.18**	**6.12 (< .0001)**
		DAN_{t-2}	0.03	0.13	0.24 (.806)
		$Estradiol_{t-2}$	**-0.48**	**0.18**	**-2.65 (.007)**
			R^2 = 0.67 (*p* = .0001); *RMSE* = 0.59 (*p* = .0009)		

Note. p-values empirically-derived via 10,000 iterations of nonparametric permutation testing.

Table 3. Vector autoregressive models for global efficiency.

Network	Outcome	Predictor	Estimate	*SE*	*T* (*p*)
Default Mode	Efficiency	Constant	0.04	0.15	0.28 (.279)
		DMN_{t-1}	-0.04	0.16	-0.27 (.764)
		$Estradiol_{t-1}$	**0.98**	**0.23**	**3.37 (.0003)**
		DMN_{t-2}	-0.02	0.16	-0.11 (.907)
		$Estradiol_{t-2}$	**-0.93**	**0.23**	**-4.00 (.002)**
			R^2 = 0.50 (*p* = .003); *RMSE* = 0.70 (*p* = .022)		
	Estradiol	Constant	0.01	0.12	0.09 (.729)
		DMN_{t-1}	-0.12	0.13	-0.95 (.339)
		$Estradiol_{t-1}$	**1.15**	**0.19**	**6.15 (< .0001)**
		DMN_{t-2}	-0.01	0.13	-0.08 (.930)
		$Estradiol_{t-2}$	**-0.48**	**0.19**	**-2.50 (.012)**
			R^2 = 0.67 (*p* < .0001); *RMSE* = 0.58 (*p* = .0004)		
Dorsal Attention	Efficiency	Constant	0.01	0.16	0.08 (.783)
		DAN_{t-1}	-0.11	0.18	-0.60 (.562)
		$Estradiol_{t-1}$	**0.84**	**0.25**	**3.35 (.002)**
		DAN_{t-2}	-0.10	0.18	-0.58 (.571)
		$Estradiol_{t-2}$	**-0.67**	**0.16**	**-2.57 (.017)**
			R^2 = 0.37 (*p* = .022); *RMSE* = 0.77 (*p* = .023)		
	Estradiol	Constant	0.01	0.12	0.06 (.808)
		DAN_{t-1}	-0.17	0.13	-1.29 (.207)
		$Estradiol_{t-1}$	**1.17**	**0.19**	**6.30 (< .0001)**
		DAN_{t-2}	-0.02	0.13	-0.16 (.875)
		$Estradiol_{t-2}$	**-0.48**	**0.19**	**-2.49 (.011)**
			R^2 = 0.68 (*p* < .0001); *RMSE* = 0.57 (*p* = .0004)		

Note. p-values empirically-derived via 10,000 iterations of nonparametric permutation testing.

List of Figures

Figure 7 | Behavioral variation across the 30-day experiment. a) Correlation plot showing relationships between mood, lifestyle measures, and sex steroid hormone concentrations. Cooler colors indicate negative correlations, warm colors indicate positive correlations, and white colors indicate no relationship. Asterisks indicate significant correlation, FDR-corrected ($q < .05$). **b)** Mood and lifestyle measures vary across the cycle. 'Day 1' indicates first day of menstruation. Abbreviations: LH = Luteinizing hormone, FSH = Follicle-stimulating hormone.

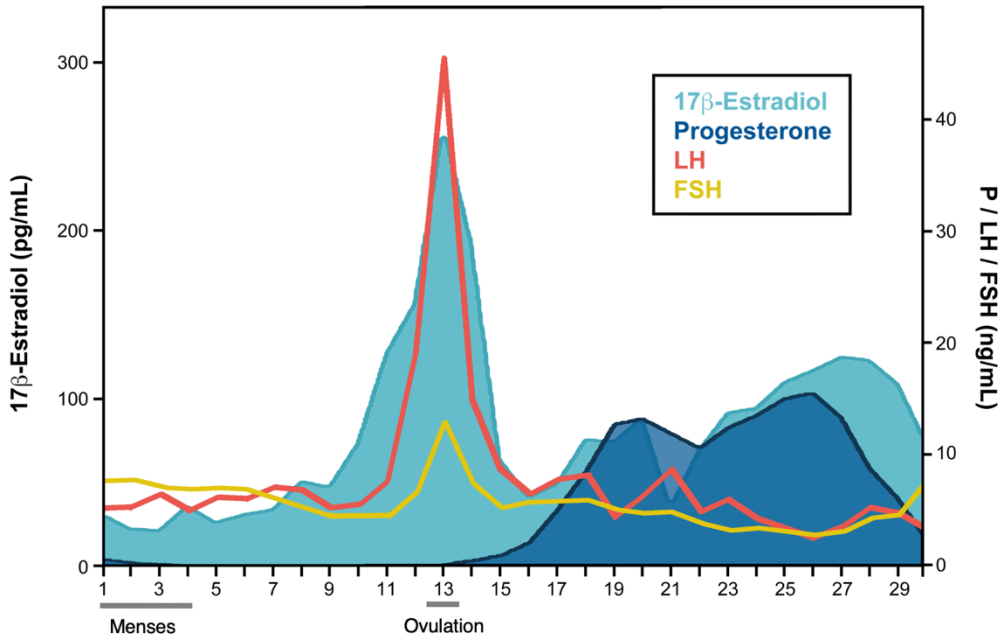

Figure 1. Participant's hormone concentrations plotted by day of cycle. 17β-estradiol, progesterone, luteinizing hormone (LH), and follicle stimulating hormone (FSH) concentrations fell within standard ranges.

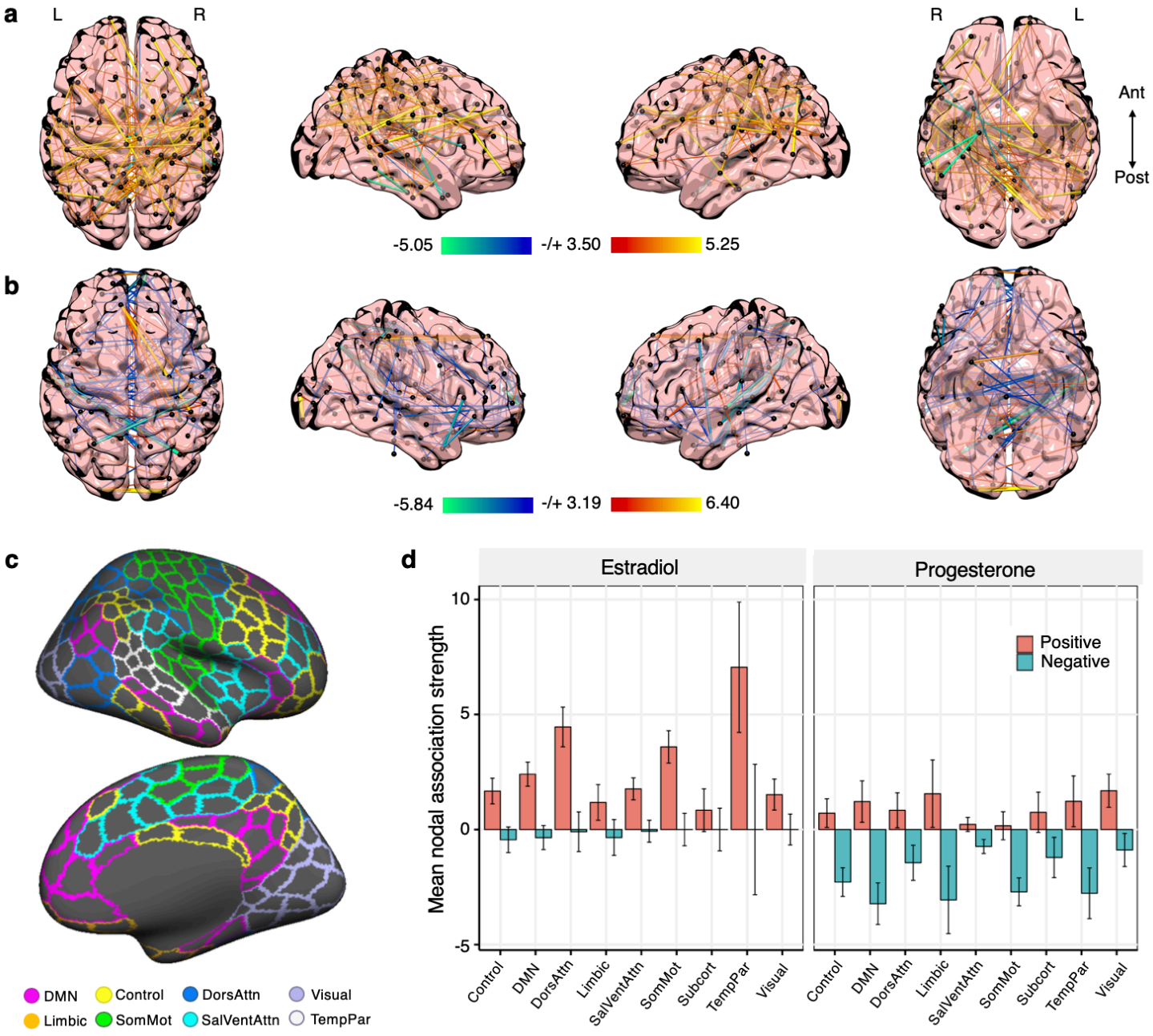

Figure 2. Whole-brain functional connectivity at rest is associated with intrinsic fluctuations in estradiol and progesterone. a) Time-synchronous (i.e. day-by-day) associations between estradiol and coherence. Hotter colors indicate increased coherence with higher concentrations of estradiol; cool colors indicate the reverse. Results are empirically-thresholded via 10,000 iterations of nonparametric permutation testing ($p < .001$). Nodes without significant edges are omitted for clarity. **b)** Time-synchronous associations between progesterone and coherence. Hotter colors indicate increased coherence with higher concentrations of progesterone; cool colors indicate the reverse. **c)** Cortical parcellations were defined from the 400-node Schafer atlas (shown here). An additional 15 subcortical nodes were defined from the Harvard-Oxford atlas. **d)** Mean nodal association strengths by network and hormone. Error bars give 95% confidence intervals. Abbreviations: DMN = Default Mode Network; DorsAttn = Dorsal Attention Network; SalVentAttn = Salience/Ventral Attention Network; SomMot = SomatoMotor Network; TempPar = Temporal Parietal Network.

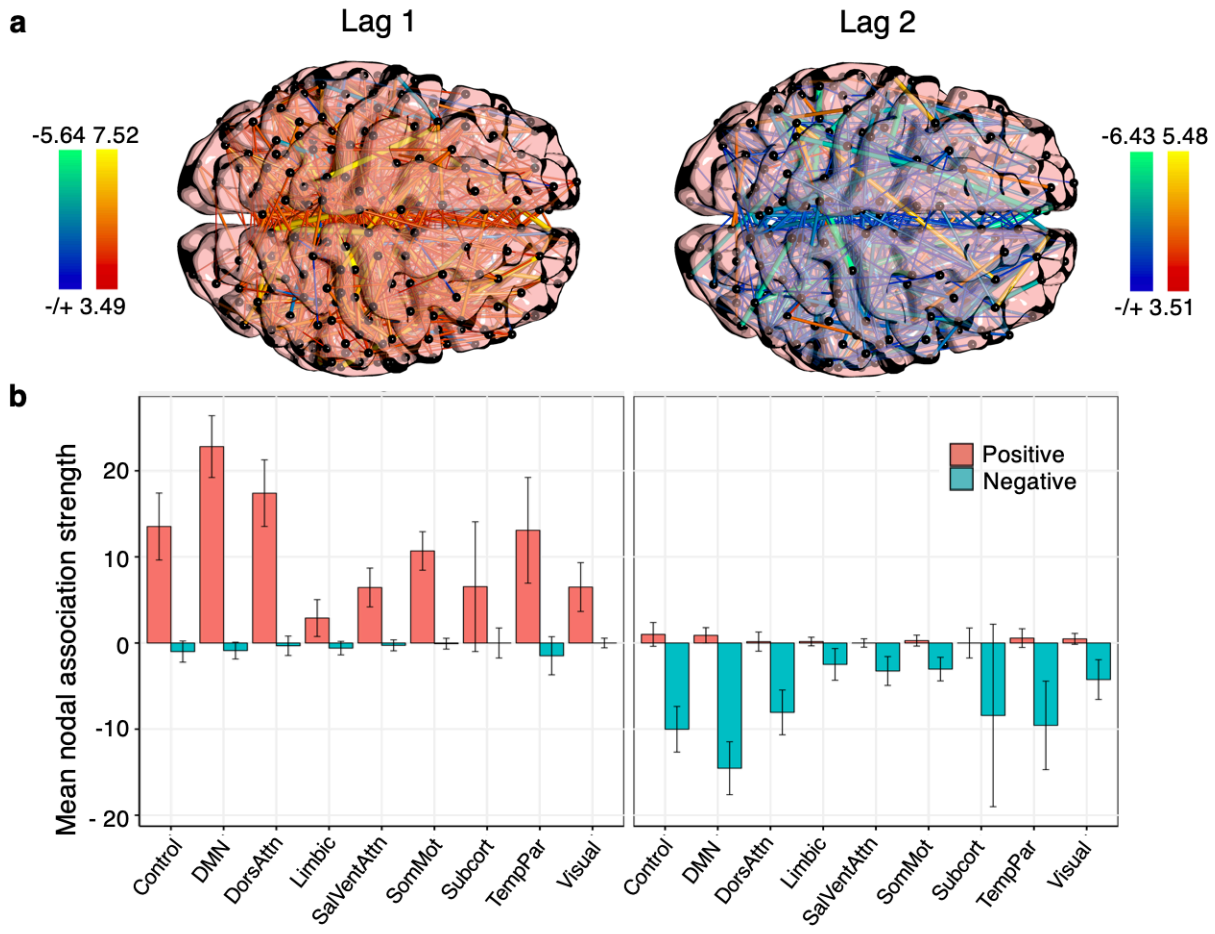

Figure 3. Whole-brain functional connectivity is linearly dependent on previous states of estradiol. a) Time-lagged associations between coherence and estradiol at lag 1 (*left*) and lag 2 (*right*), derived from edgewise vector autoregression models. Hotter colors indicate a predicted increase in coherence given previous concentrations of estradiol; cool colors indicate the reverse. Results are empirically-thresholded via 10,000 iterations of nonparametric permutation testing ($p < .001$). Nodes without significant edges are omitted for clarity. **b)** Mean nodal association strengths by network and time lag. Error bars give 95% confidence intervals.

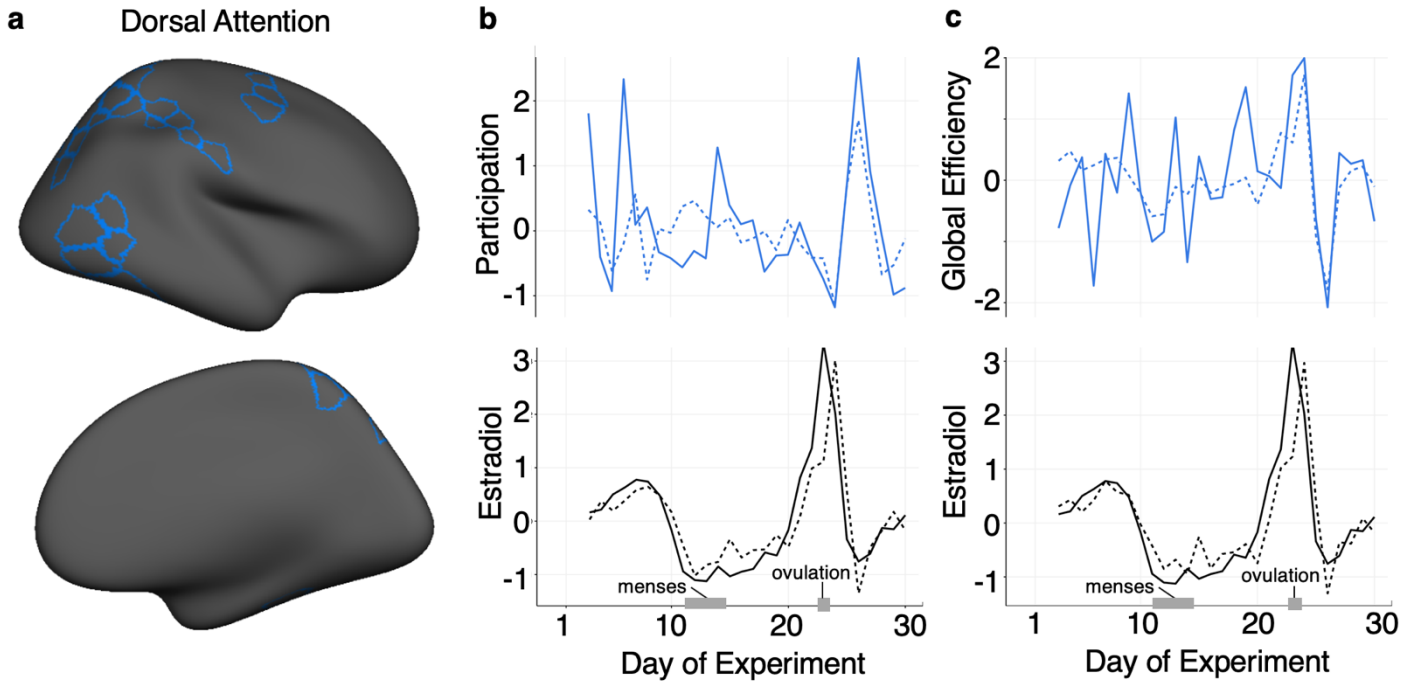

Figure 4. Dorsal Attention Network topology is driven by previous states of estradiol. Observe data (*solid lines*) vs. VAR model fits (*dotted lines*) for between-network participation (**b**, *middle*) and within-network efficiency (**c**, *right*) in the Dorsal Attention Network (**a**, *left*). Timeseries for each network statistic are depicted *above* in b,c and estradiol for each VAR is plotted *below*. Data are in standardized units and begin at experiment day three, given the second-order VAR (lag of two days).

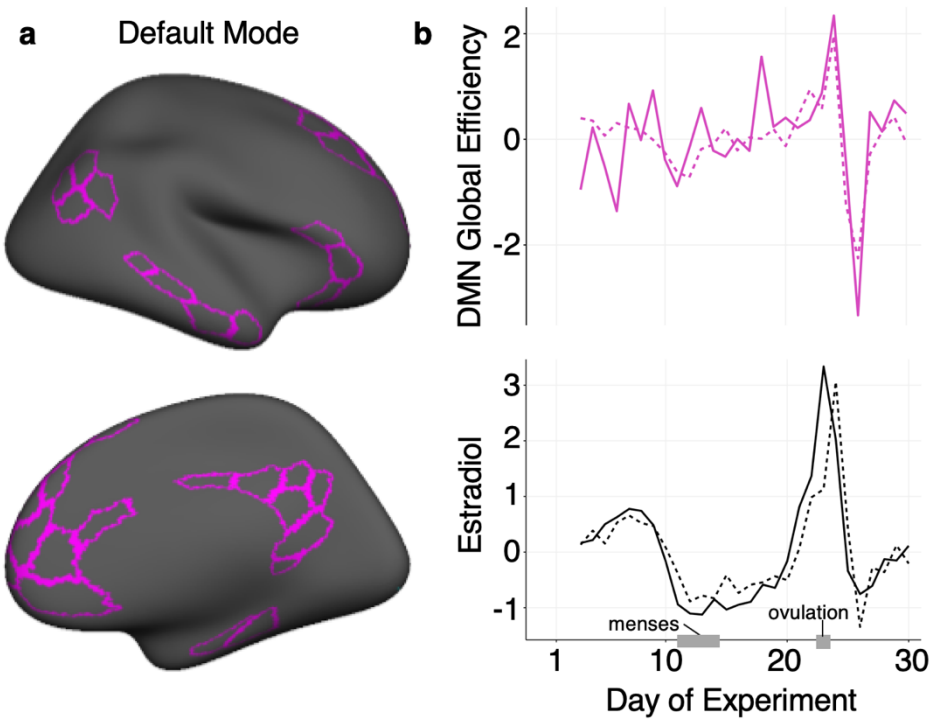

Figure 5. Default Mode Network topology is driven by previous states of estradiol. Observed data (*solid lines*) vs. VAR model fits (*dotted lines*) for within-network efficiency (**b**, *right*) in the Default Mode Network (**a**, *left*). The efficiency timeseries is depicted *above* in **b** and estradiol is plotted *below*. Data are in standardized units and begin at experiment day three, given the second-order VAR (lag of two days).

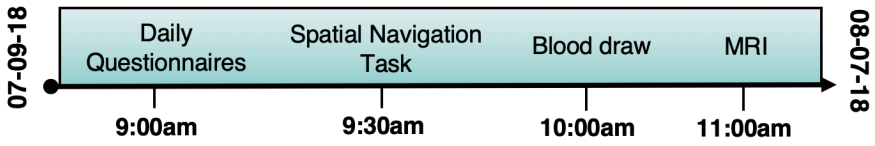

Figure 6. Timeline of data collection for the 30 experimental sessions. Endocrine and MRI assessments were collected at the same time each day to minimize time of day effects.

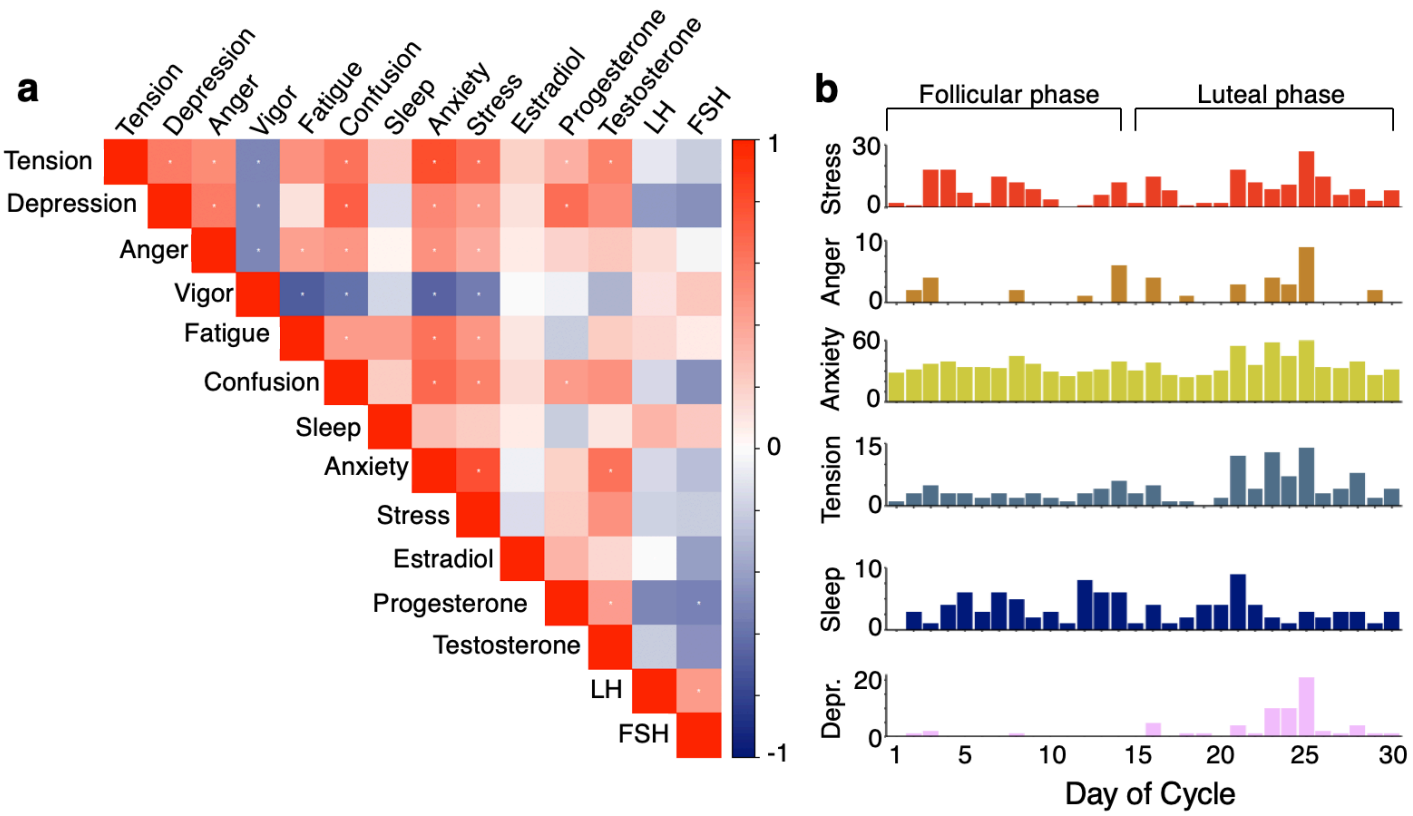

Figure 7. Behavioral variation across the 30 day experiment. a) Correlation plot showing relationships between mood, lifestyle measures, and sex steroid hormone concentrations. Cooler colors indicate negative correlations, warm colors indicate positive correlations, and white colors indicate no relationship. Asterisks indicate significant correlation, FDR-corrected ($q < .05$). **b)** Mood and lifestyle measures vary across the cycle. 'Day 1' indicates first day of menstruation, *not* first day of experiment. Abbreviations: LH = Luteinizing hormone, FSH = Follicle-stimulating hormone.